

# CASSBEAM

Software for Cassegrain antenna modelling

Walter Briskeen

National Radio Astronomy Observatory

Version 1.0

August 18, 2003

## 1 Introduction

Cassbeam is a Cassegrain antenna ray tracer. Based on an input text file, it computes several properties of the antenna including gain, zenith system temperature, and the beam, in full polarization. All calculations are done in the *transmit sense* and use reciprocity to relate to the equivalent receiving system.

A classical Cassegrain antenna consists of a paraboloidal primary optical surface and a hyperboloidal secondary. This allows a large effective focal length to be shortened considerably. This means that more directive feeds can be used. Since wideband feeds tend to have narrower radiation patterns, the Cassegrain is often a better choice for wide band systems. A second advantage of Cassegrain systems is that the radiation that spills over the secondary reaches the cold sky rather than the 290K ground. Shaped Cassegrain systems have primary surfaces that are rotationally symmetric but no longer paraboloidal. The secondary is then shaped as well in order to well define a secondary focus. Shaping is used to adjust the amplitude of the illumination across the primary, allowing for higher aperture efficiency. An additional deviation from the classical Cassgrain is placing the feed off axis and compensating with an asymmetric secondary. This is used at the VLA. It allows a rotation of the subreflector about the primary's symmetry axis to point the beam toward one of six feeds. Both of these deviations from a classical Cassegrain are supported. An example of a offset, shaped Cassegrain antenna is shown in Fig. 1. Additionally, cassbeam allows deformations, or "pathologies" of the optics to be modelled. Currently this is limited to rotations and translations of the feed and secondary. In the future, large scale deviations in the primary (such as a misplaced panel) will likely be supported.

This software is presented to the world under the Gnu General Public License (GPL) version 2.0<sup>1</sup>. The use of this software is at your risk! Although this software is thought to produce correct output, your mileage may vary.

### 1.1 Sample use case

Here is a very terse description on how to use cassbeam. Read this entire document to understand what is actually happening. First an input file must be created. A sample input file called `X-mid.in` is shown in Appendix A. This file specifies the geometry of the EVLA antenna and has some parameters tuned for X-band in particular. A second file must also be created called `vla_geom` to supply the shape of the primary. A portion of this file is shown in Appendix B. Cassbeam is run simply by supplying the input filename. A sample session is shown in Appendix C. Running this file produces 12 output files that will be explained in detail in Sec. 3.3.

### 1.2 Limitations

In its current form, cassbeam only computes the properties of Cassegrain antennas that have a rotationally symmetric primary surface. The figure of this primary may be specified as a function of radius. While all  $z(r)$  curves are legal input, pathological surfaces (such as those with negative  $z'(r)$ ) will either produce non-physical results or will cause abnormal program termination. Gregorian geometries, those where the secondary surface is concave and above the prime focus, will probably produce correct answers but this geometry is not formally supported.

---

<sup>1</sup>See <http://www.gnu.org/copyleft/gpl.html> or the LICENSE file included with the software for more information.

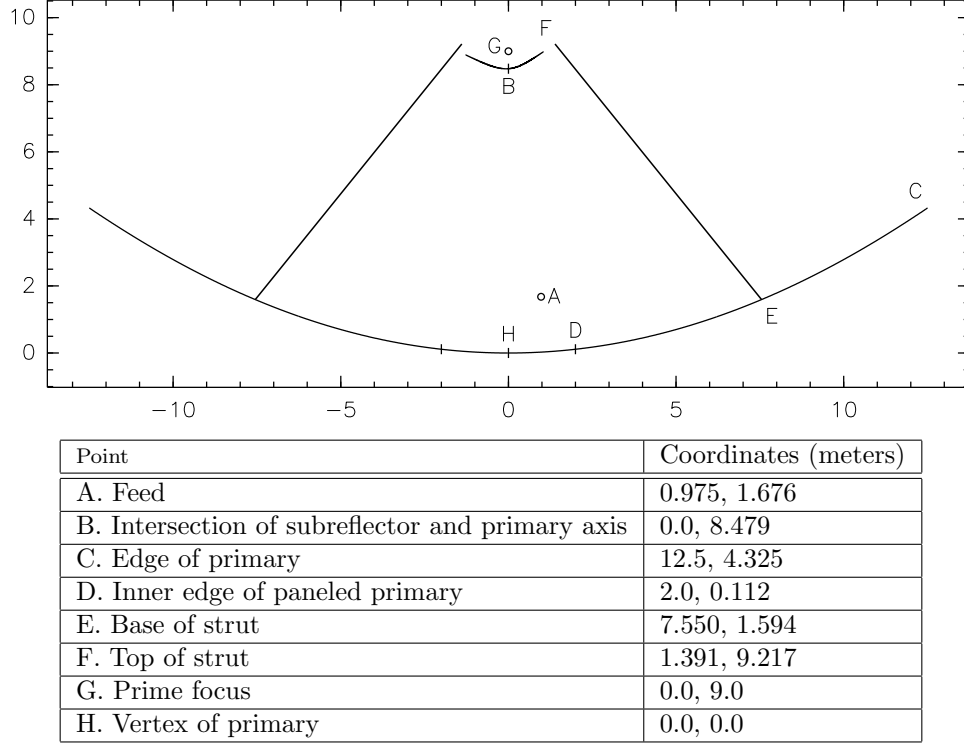


Figure 1: The VLA antenna optics. This is an example of a shaped, offset Cassegrain. Coordinates are  $x, z$ .

The number of struts (secondary supports) is currently fixed to be four. This will likely change with future versions of this software.

Cassbeam works in the optical regime, meaning that the wavelength is assumed to be infinitesimal. This allows the use of ray tracing rather than physical optics, which is much faster and much simpler to implement. Antenna geometries with structures with dimensions smaller than about 2 wavelengths will produce results that deviate from reality, although tests with  $1 \lambda$  struts show results that are consistent with a similar simulation using physical optics in Grasp8. Also optical surfaces with sharp edges will likely be treated incorrectly.

## 2 Conventions

In the optics world there are several examples of contradictory conventions that potentially lead to confusion. The conventions chosen here aim to be those most commonly encountered in the radio astronomy community. In most cases, these are the same as those used within antenna engineering.

### 2.1 Units

The metric system is used exclusively over imperial units. Specifically, the meter is used as the unit of length, the nanosecond is used as the unit of time, and all frequencies are measured in GHz. The user specifies angles in degrees, although within the software radians are used in all angular calculations. All temperatures are in Kelvin.

## 2.2 Coordinate systems

The user must define the coordinates of various antenna components in *antenna coordinates*. In this right-handed Cartesian coordinate system,  $\hat{z}$  points along the symmetry axis of the antenna, toward the pointing direction. Above is always taken to mean “with greater  $z$  value.” The  $\hat{x}$  direction is taken to be parallel to the ground and  $\hat{y}$  is thus determined by orthogonality.  $\hat{y}$  points away from the ground. The radial coordinate used to define the shape of the primary is  $r \equiv \sqrt{x^2 + y^2}$ . The origin of the coordinate system is the vertex of the primary – the point on the vertex that intersects the  $z$  axis.

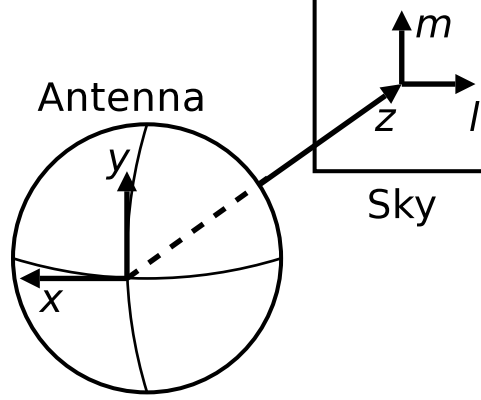


Figure 2: The antenna and sky coordinate systems. This view is from behind the primary surface looking at the sky.

The sky coordinate system is a two-dimensional sine-projected angular coordinate system used to define the beam axes. The sine-projection comes naturally out of the Fourier transform that relates the aperture field to the radiation pattern on the sky. The origin of this coordinate system is the pointing direction,  $\hat{z}$ . At this point,  $\hat{l}$  points parallel to  $-\hat{x}$  and  $\hat{m}$  is parallel to  $\hat{y}$ . In other words,  $\hat{l}$  points west and  $\hat{m}$  points north when the antenna is pointed at the meridian.

## 2.3 Fields

The vacuum plane wave solutions to Maxwell’s equations are harmonic in time. Internally, complex notation is used in field calculations, which simplifies notation and allows temporal and spatial evolution of the plane wave fields to be expressed with complex exponentials. The physical field is the real component of its complex value. Both sign conventions are used for the phase factor. The convention used by both Jackson and Thompson, Moran, and Swenson is used; the evolution of plane wave fields is governed by

$$\vec{E}(\vec{x}, t) = \vec{E}_0 e^{i(\vec{k} \cdot \vec{x} - 2\pi\nu t)}. \quad (1)$$

Note that Born and Wolf use the opposite convention for the phase (and thus also for circular polarization). Here  $\vec{k}$  is the wave vector (with magnitude  $2\pi/\lambda$ ) and  $\nu$  is the frequency (cycle rate).  $\vec{E}_0$  is a vector quantity with magnitude equal to the electric field strength. The direction of the vector describes its polarization state. The electric field is transverse:

$$\vec{k} \cdot \vec{E}_0 = 0. \quad (2)$$

For completeness, it is noted that the magnetic induction is given by

$$\vec{B} = \frac{c}{|k|} \vec{k} \times \vec{E}. \quad (3)$$

## 2.4 Polarization

A right handed linear polarization coordinate system is used. The linear polarization basis unit vectors used,  $\mathbf{e}_1$  and  $\mathbf{e}_2$ , depend on the direction of propagation,  $\mathbf{e}_3$ , but always have the following orthogonality properties:

$$\mathbf{e}_i^* \cdot \mathbf{e}_j = \delta_{ij} \quad (4)$$

$$\mathbf{e}_1 \times \mathbf{e}_2 = \mathbf{e}_3 \quad (5)$$

The IEEE definition of circular polarization is used. With the above phase convention (Eqn. 1), the right and left circular polarization basis vectors are respectively

$$\mathbf{e}_R = \frac{1}{\sqrt{2}}(\mathbf{e}_1 + i\mathbf{e}_2) \quad (6)$$

$$\mathbf{e}_L = \frac{1}{\sqrt{2}}(\mathbf{e}_1 - i\mathbf{e}_2). \quad (7)$$

Note that these two unit vectors and  $\mathbf{e}_3$  satisfy the orthogonality condition of Eqn. 4. A useful property of the circular polarization basis vectors is that they are eigenvectors of  $\mathbf{e}_3 \times$  with eigenvalues  $-i$  and  $i$  for  $\mathbf{e}_R$  and  $\mathbf{e}_L$  respectively. Thus since  $\vec{k} = k\mathbf{e}_3$ ,

$$\vec{k} \times \mathbf{e}_R = -ik\mathbf{e}_R \quad (8)$$

$$\vec{k} \times \mathbf{e}_L = ik\mathbf{e}_L \quad (9)$$

The ‘1’ polarization vector in radio astronomy is often taken to be that which points toward the meridian (see Fig. 3). Thus for a receiving system,  $\mathbf{e}_1 \propto \hat{m}$ ,  $\mathbf{e}_2 \propto -\hat{l}$ , and  $\mathbf{e}_3 \propto -\hat{z}$ . To avoid confusion  $\mathbf{e}_1$  and  $\mathbf{e}_2$  are used in lieu of the explicit Cartesian axes,  $\mathbf{e}_x$  and  $\mathbf{e}_y$ .

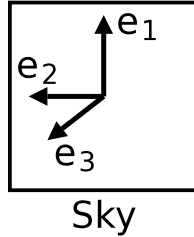


Figure 3: The polarization basis vectors. Note that  $\mathbf{e}_3$  points out of the page, toward the antenna.

## 2.5 The Stokes parameters

The Stokes parameters provide a compact representation of the statistical properties of the polarization of quasi-monochromatic or broad-band radiation. The 4 parameters are most often labeled  $I$ ,  $Q$ ,  $U$ , and  $V$ , although other conventions, such as  $\{s_0, s_1, s_2, s_3\}$  and  $\{A, B, C, D\}$  also exist. The Stokes parameters are defined by the following linear polarization products:

$$I = \langle E_1^* E_1 \rangle + \langle E_2^* E_2 \rangle \quad (10)$$

$$Q = \langle E_1^* E_1 \rangle - \langle E_2^* E_2 \rangle \quad (11)$$

$$U = 2\Re \langle E_1^* E_2 \rangle \quad (12)$$

$$V = 2\Im \langle E_1^* E_2 \rangle \quad (13)$$

They are equally well defined by circular polarization products:

$$I = \langle E_R^* E_R \rangle + \langle E_L^* E_L \rangle \quad (14)$$

$$Q = \langle E_R^* E_R \rangle - \langle E_L^* E_L \rangle \quad (15)$$

$$U = 2 \Re \langle E_R^* E_L \rangle \quad (16)$$

$$V = 2 \Im \langle E_R^* E_L \rangle \quad (17)$$

In these equations,  $E_i \equiv \mathbf{e}_i^* \cdot \vec{E}$  for any polarization component  $i$  in  $\{1, 2, R, L\}$ . The symbols  $\Re$  and  $\Im$  extract the real and imaginary part of a complex number, respectively.

## 2.6 Additional terminology

Here we list some other terminology that will be useful in the following sections.

**aperture plane** The surface in the  $x - y$  plane containing the rim of the primary.

**struts** The secondary supports, or legs.

## 3 User reference

The user provides inputs to `cassbeam` through an input file. Additional options can be passed to `cassbeam` on the command line. Based on the arguments to the **command** parameter, various output files are generated in addition to the text dumped to the screen.

### 3.1 Input files

The main input file consists of a series of lines of the form *key = value*. Only one such entry is allowed per line. The equal sign is optional. The input files allow comments to be placed within the file. All comments begin with `%`. This character and any that follow it on a given line are ignored by `cassbeam`. Depending on *key*, the *value* may be one of five types: string, integer, double, vector, none. A string is a sequence of non-whitespace characters *not* surrounded by quotes of any kind. A double value is a number that can have a fractional part. A vector is a comma-separated list of doubles. The ‘none’ type expects no *value*. Below is a list of the allowed *keys* and the type of *value* expected. If the range of legal values is restricted, the legal range will be contained within brackets. Note that legal values do not imply a physical system that will generate meaningful results! For the vector type, if a certain number of values are needed, they will be indicated in parentheses. A required parameter will be indicated with a ‘\*’. It is important to realize that the secondary optical surface (i.e., the subreflector) is defined based on the input geometry. Thus changing the feed placement will change the geometry of the subreflector! To change parameters of the telescope without affecting the shape of the subreflector, set the pathology parameters. Note that the order of the parameters does not matter.

#### 3.1.1 Antenna geometry parameters

**feed\_x** *double*

The  $x$  value of the phase center of the feed. If no value is provided, 0 is assumed.

**feed\_y** *double*

The  $y$  value of the phase center of the feed. If no value is provided, 0 is assumed.

**feed\_z** *double*

The  $z$  value of the phase center of the feed. If no value is provided, 0 is assumed.

**geom\*** *string*

This string points to a disk file containing the primary optical surface geometry. This file is a three column ascii text file, each containing space separated values for  $r$ ,  $z$ , and  $dz/dr$  for the antenna. There is no limit (other than your computer's memory) to the number of lines in this file. It is assumed (but not checked!) that the values of  $r$  start at 0 and are equally spaced. The radius,  $R$ , of the primary is given by the value of  $r$  in the last row. Columns 1 and 2 are in meters, and column 3 is dimensionless.

**hole\_radius** *double* [ $> 0$ ]

The radius (in meters) of an unpanelled area at the center of the primary. If omitted, no hole will be made.

**legapex** *double* [ $> 0$ ]

The  $z$  value where the legs (struts) intersect each other. Note that the legs might terminate before reaching this point. The default value is  $1.2 \times \text{sub\_h}$ .

**legfoot** *double* [ $> 0$ ]

The  $r$  value where the legs (struts) intersect the primary surface. The default value is half the antenna radius.

**legwidth** *double*

The effective width of the legs, used to compute blockage. Note that currently a positive value indicates four equally spaced legs with one leg along the  $x$  axis. If the value is negative, its absolute value is used in the blockage calculations, but the legs are rotated  $45^\circ$ . If this parameter is not set, or if it is set to 0, then no legs will be generated.

**name** *string*

An optional name given to the antenna. If the name is "VLBA", then the true strut geometry for the VLBA antennas is used rather than equispaced struts.

**roughness** *double* [ $/ge 0$ ]

The RSS surface roughness in meters. This number represents the combined surface error for the primary and secondary. If no roughness is provided, the default value of 0 is used.

**sub\_h\*** *double* [ $> 0$ ]

This value is the  $z$  value of the intersection of the subreflector with the  $z$  axis.

### 3.1.2 Feed pattern parameters

Note that either both **feedtaper** and **feedangle** or **feedpattern** must be provided.

**feedangle** *double* [ $> 0$ ]

Sets the reference angle for the feed taper.

**feedpattern** *string*

The name of the file containing the pattern of the feed. This file contains two space-separated columns of numbers: the angle in degrees and the taper in dB. The first angle must equal 0, and the angles must be uniformly spaced.

**feedpatternscale** *double* [ $> 0$ ]

The factor by which to scale the pattern defined in **feedpattern**.

**feedtaper** *double* [ $> 0$ ]

This parameter sets the taper (in dB) of the feed at an angle **feedangle** from the feed axis to  $10^{-\text{feedtaper}/10}$ .

### 3.1.3 Pathology parameters

None of the following operations change the shape of the subreflector – its geometry is calculated before their application. Note that displacements of either the feed or the subreflector result in a rotation of the feed that corrects for the mispointing caused by the translations. Rotations of the feed act in addition to this correction. Compositing rotations (i.e., setting **rsub\_x** and **rsub\_y** are both provided), the operations on the object being rotated proceed in reverse alphabetical order (*z* rotation before *y* rotation; *y* rotation before *x* rotation) regardless of the order that the parameters are received.

**dfeed\_x** *double*

Displacement of the feed along the *x* axis.

**dfeed\_y** *double*

Displacement of the feed along the *y* axis.

**dfeed\_z** *double*

Displacement of the feed along the *z* axis.

**dsub\_x** *double*

Displacement of the subreflector along the *x* axis.

**dsub\_y** *double*

Displacement of the subreflector along the *y* axis.

**dsub\_z** *double*

Displacement of the subreflector along the *z* axis.

**focus** *double*

Displacement of the feed along the feed axis. A positive value moves the feed closer to the subreflector.

**rfeed\_x** *double*

Rotation of the feed in degrees about the *x* axis. A positive value will rotate from the *z* axis through the *y* axis.

**rfeed\_y** *double*

Rotation of the feed in degrees about the *y* axis. A positive value will rotate from the *x* axis through the *z* axis.

**rfeed\_z** *double*

Rotation of the feed in degrees about the *z* axis. A positive value will rotate from the *y* axis through the *x* axis.

**rsub\_x** *double*

Rotation of the subreflector in degrees about the *x* axis. A positive value will rotate from the *z* axis through the *y* axis.

**rsub\_y** *double*

Rotation of the subreflector in degrees about the *y* axis. A positive value will rotate from the *x* axis through the *z* axis.

**rsub\_z** *double*

Rotation of the subreflector in degrees about the *z* axis. A positive value will rotate from the *y* axis through the *x* axis.

**subrotpoint** *vector (1 or 2 or 3)*

Defines the point about which the rotation of the subreflector is performed. The contents of the vector depend on the number of elements are provided:

1. The  $z$  value;
2. The  $x$  and  $y$  values;
3. The  $x$ ,  $y$ , and  $z$  values.

### 3.1.4 Operating condition parameters

**compute** *string* ['all' or 'none' or combination of 'a', 'j', 'p', & 's']

A string to tell what output to produce. The string can be 'all', 'none', or a string containing flag characters. The default value is 'all', meaning produce all possible output. 'none' will produce only messages on the screen and no output files. The characters of the general string mean the following:

- a** Save the aperture images;
- j** Save the Jones matrices in a table;
- p** Save the parameters;
- s** Save the polarized beams.

Note that the string is case insensitive. See Sec. 3.3 for an explanation of the output files.

**diffeff** *double*

A user supplied diffraction efficiency. If none is provided, an internal algorithm that is not very good is used. This needs to be upgraded!

**freq\*** *double* [ $> 0$ ]

The frequency in GHz at which the calculation will be run.

**gridsize** *integer* [ $\geq 32$ ]

Specifies a fixed grid size. If odd, the next even number will be used. This option overrides any setting of **oversamp** and is the preferred method of setting the grid size. Setting it to a value less than 32 will result in a grid size of 32.

**leggroundscatter** *double* [ $\geq 0, \leq 1$ ]

The fraction of power that scatters off the struts toward the ground. The default value is 0.2.

**misceff** *double* [ $\geq 0, \leq 1$ ]

A factor of the efficiency calculation that contains "everything else". The user is responsible for choosing a realistic value for this. A default of 1 (i.e., 100%) is assumed if this parameter is not provided.

**out** *string*

The prefix for all output files. The default is *cassbeam*. A dot will always separate the prefix from any trailing characters.

**oversamp** *double* [ $> 0$ ]

One way of specifying the grid size. This option will make the grid on the primary fine enough to accommodate  $4 \cdot \text{oversamp} \cdot R / \lambda$  points. The default is 1. Note that vastly "undersampling" is fine as the field is never calculated anywhere between the feed and the aperture plane. Normally blockage calculations and constancy of the illumination will dictate the required sampling. See **gridsize** for an alternate way of specifying the grid. This parameter is ignored if **gridsize** is set.

**pixelsperbeam** *int* [ $> 0$ ]

This is the approximate number of pixels that the core of the beam will occupy in the output images.

**Tground** *double* [ $> 0$ ]

The temperature in Kelvin of the ground. The default value is 290.



**Trec** *double* [ $> 0$ ]

The equivalent temperature of the receiver. This adds into the system temperature. The default value is 50.

**Tsky** *double* [ $> 0$ ]

The temperature in Kelvin of the sky. The default value is 3 for frequencies over 1 GHz, and  $3 \times 10^{-2.5\nu}$  for frequencies below 1 GHz.

## 3.2 Running cassbeam

Cassbeam is a non-interactive command line program that takes all of its input from the command line. Note that this does not preclude someone at a later date from making a graphical or web front end. There is one required argument when running cassbeam – the input filename that is described above in Sec/ 3.1. Additional arguments can supplement the parameters of the input file. These arguments are passed in the same *key=value* as required in the input file *except* whitespace is not allowed around the equal sign. If a parameter appears both in the input file and the command line, then the value on the command line supercedes the value on the input file.

## 3.3 Output files

Up to 12 output files are generated with version 1.0 of cassbeam depending on which **compute** options were selected at run time. These files are listed below. The letter in brackets in the section headings indicate which option is used to enable this file to be written. All output files begin with the value of the input parameter **out**. Currently all output images are in **.pgm**<sup>2</sup> format, which is a very simple greyscale image format supported by most unix-based image viewers.

### 3.3.1 Aperture images [a]

Three images are generated that allow the aperture field to be examined qualitatively. If quantitative numbers are needed, the source code should be modified to export the illumination parameters.

- **out.illumamp.pgm** is a raster image showing the amplitude of the illumination pattern of the primary. No blockage is done at this point. The scale is linear in flux.
- **out.illumphase.pgm** is a raster image showing the net phase (pathlength multiplied by wave vector) at each point on the primary. A phase gradient is removed. Portions of the image that correspond to zero flux have an arbitrary phase.
- **out.illumblock.pgm** is a raster image showing the blocked portion of the aperture. White means that this part of the dish is experiences either plane wave blockage from the sky or spherical wave blockage from the feed, and thus does not contribute to the gain of the antenna.

### 3.3.2 Jones matrix file [j]

The Jones matrix file, **out.jones.dat** contains the Jones matrix (see Hamaker et al. 1996 for details) corresponding to the effect of the antenna on the incoming radiation as a function of position on the sky. The file is organized as an eight column ascii with columns  $\{\Re g_{RR}, \Im g_{RR}, \Re g_{LR}, \Im g_{LR}, \Re g_{RL}, \Im g_{RL}, \Re g_{LL}, \Im g_{LL}\}$ . The first row corresponds to the point on the image with smallest  $l$  and  $m$ . The rastering then proceeds first with increasing  $l$ , and then with increasing  $m$ . There are a total of  $n^2$  rows, where  $n$  is the smallest odd number greater than or equal to the **gridsize** used. The matrices are rastered on a sine-projected coordinate system tangent to the sky at the beam center, which corresponds to row number  $(n^2 + 1)/2$ . At the beam center the pixel scale is given by the output parameter **beampixelscale**, which is stored in the output file **out.params** described below.

---

<sup>2</sup>See <http://www.die.net/doc/linux/man/man5/pgm.5.html> for details on this format.

### 3.3.3 Parameter file [p]

The parameter file, **out.params** is an output file in the same format as the input file, containing all of the input parameters that were specified (even if on the command line) as well as many output values. They are:

**Aeff** *double*

The effective area of the antenna [ $\text{m}^2$ ].

**Aeff\_Tsys** *double*

The effective area of the antenna divided by the system temperature [ $\text{m}^2/\text{K}$ ].

**ampeff** *double*

The amplitude efficiency,  $\eta_{\text{I,amp}}$ .

**beampixelscale** *double*

The scale of the generated beam images [ $\text{deg/pixel}$ ].

**blockeff** *double*

The blockage efficiency,  $\eta_{\text{B}}$ .

**diffeff** *double*

The diffraction efficiency,  $\eta_{\text{D}}$ .

**fwhm\_l** *double*

The full width at half max of the beam in the  $l$  direction.

**fwhm\_m** *double*

The full width at half max of the beam in the  $m$  direction.

**gain** *double*

The gain  $G$  of the antenna, as defined by Eqn. 20.

**illumeff** *double*

The illumination efficiency,  $\eta_{\text{I}}$ .

**peaksidelobe** *double*

The directivity of the greatest sidelobe relative to the peak directivity of the beam.

**phaseeff** *double*

The phase efficiency,  $\eta_{\text{I,phase}}$ .

**point\_l** *double*

The  $l$  component of the pointing offset from the  $z$  axis measured in the image plane.

**point\_m** *double*

The  $m$  component of the pointing offset from the  $z$  axis measured in the image plane.

**prispilleff** *double*

The primary spillover efficiency,  $\eta_{\text{S,pri}}$ .

**program** *string*

The name of the program run, which is **cassbeam**.

**misceff** *double*

The miscellaneous efficiency,  $\eta_{\text{M}}$ .

**spilleff** *double*

The spillover efficiency,  $\eta_{\text{S}}$ .

**subspilleff** *double*

The subreflector spillover efficiency,  $\eta_{S,\text{sub}}$ .

**surfeff** *double*

The surface efficiency, given by Eqn. 27.

**totaleff** *double*

The total efficiency calculated for the antenna, given by Eqn. 21.

**Tsys** *double*

The system temperature calculated with Eqn. 32.

**version** *string*

The software version number.

### 3.3.4 Polarized beam images [s]

With the **s** option, cassbeam will produce 7 images of the beam showing in the four Stokes parameters the response to an unpolarized source as a function of the position of the source on the sky. This information is derived from the Jones matrices which are saved in **out.jones.dat**. These images are meant for qualitative inspection. The Jones matrices contain the formal output.

- **out.I.pgm** Stokes  $I$  – total intensity;
- **out.Q.pgm** Stokes  $Q$  – excess linear polarization in  $\mathbf{e}_1$  over  $\mathbf{e}_2$ ;
- **out.U.pgm** Stokes  $U$  – excess linear polarization in  $\mathbf{e}'_1$  over  $\mathbf{e}'_2$ <sup>3</sup>;
- **out.V.pgm** Stokes  $V$  – excess right circular polarization over left circular polarization;
- **out.QI.pgm** The ratio of the Stokes  $Q$  image to the Stokes  $I$  image;
- **out.UI.pgm** The ratio of the Stokes  $U$  image to the Stokes  $I$  image;
- **out.VI.pgm** The ratio of the Stokes  $V$  image to the Stokes  $I$  image;

## 4 Theory of operation

This section briefly describes how the code works. Many details are left out. See the source code if further understanding is needed.

### 4.1 Ray tracing

Ray tracing is used to determine the electric field at each grid point on the aperture plane. This is done through a complicated process that will be discussed briefly here. For each grid cell on the primary, the following process is followed.

We are interested in calculating the electric field on a uniformly spaced grid on the aperture plane. Since the ray may not travel along  $\hat{z}$  from the primary to the aperture plane, some iteration is required. First the  $(x, y)$  position of the grid point to be calculated is taken as the starting point on the primary. The corresponding  $z$  value and the surface normal are then calculated for that point on the primary. The virtual ray is then reflected off the subreflector. It should be noted here that nowhere is the subreflector ever stored as a rastered surface – it is recomputed each time it is needed, and this is likely far more efficient than searching a tabulated surface for an intersection point. The subreflector displacement and rotation are then considered. A ray is then projected from the feed to this point on the subreflector. The process is reversed

---

<sup>3</sup> $\mathbf{e}'_1 = 1/\sqrt{2}(\mathbf{e}_1 + \mathbf{e}_2)$ ,  $\mathbf{e}'_2 = 1/\sqrt{2}(\mathbf{e}_2 - \mathbf{e}_1)$

now that a guess for the appropriate subreflector point is made. A ray is traced from the feed to this point on the subreflector, reflected toward the primary, and finally reflected to the aperture plane. The  $(x, y)$  value of the intersection of the ray with the aperture plane is compared with the initial  $(x, y)$ . An offset is applied to the original value and the iteration continues. About 3 iterations are sufficient for convergence, although about 7 are done in practice.

Once points on both the aperture plane and the primary are known, the final ray is defined. Three rays are shot out from a small triangular region of the aperture plane and are used to calculate  $dP/dA$ , the flux through the point of interest on the aperture plane. This value includes the taper of the feed, the dilution of the beam due to expansion, and the effects of all the surface shapings. The length of the ray is then used to derive the phase of the field on the aperture. Finally, the two circular polarization vectors are propagated from the feed. Reflections obey the proper boundary conditions for a conducting surface:

$$E_{\parallel} = 0 \quad (18)$$

$$B_{\perp} = 0 \quad (19)$$

The electric field, decomposed into a linear polarization basis for each outgoing circular polarization, is computed on the aperture plane grid.

## 4.2 Antenna performance

The gain,  $G$ , is calculated by first computing the efficiency,  $\eta$ , and then using

$$G = 4\pi\eta \frac{A}{\lambda^2}. \quad (20)$$

Here  $\lambda$  is the observing wavelength, and  $A$  is the geometric area of the primary, including any unused portion. For a circular aperture,  $A = \pi R^2$ . The efficiency is computed by multiplying many factors, each with its own physical cause:

$$\eta = \eta_S \eta_B \eta_{\sigma} \eta_I \eta_D \eta_M \quad (21)$$

The meanings and definitions of these factors will be discussed below.

A useful quantity is the total power radiated by the feed, given by

$$P_{\text{total}} = \int_{4\pi} |E^2(\theta, \phi)| d\Omega. \quad (22)$$

The integral is performed over all  $4\pi$  steradians and  $\vec{E}(\theta, \phi)$  is the electric field radiated by the feed. Note that an overall constant factor of  $(4\pi)^{-1}$  is removed from this equation to simplify notation.

Of particular importance to radio astronomy is the ratio of gain to system temperature. This is directly related to the on-axis sensitivity of the antenna.

### 4.2.1 Spillover efficiency, $\eta_S$

The spillover efficiency is the fraction of power radiated that ends up illuminating the primary surface. For a two reflector system, spillover can occur at two places: around the subreflector and around the primary. In the GO limit, a perfectly aligned Cassegrain antenna will only spill around the secondary, as any ray hitting the secondary will hit the primary. For a misaligned system this is no longer strictly true. The total spillover efficiency is then a product of the subreflector spillover efficiency,  $\eta_{S,\text{sub}}$  and that of the primary,  $\eta_{S,\text{pri}}$ . The secondary spillover efficiency is calculated as:

$$\eta_{S,\text{sub}} = \frac{\int_{\text{sub}} |E^2(\theta, \phi)| d\Omega}{P_{\text{total}}}. \quad (23)$$

The numerator is the integrated power over the solid angle subtended by the subreflector. The total spillover is the fraction of power hitting the primary,

$$\eta_S = \frac{\int_{\text{aper}} |E^2(x, y)| dA}{P_{\text{total}}}. \quad (24)$$

Here  $\vec{E}(x, y)$  is the electric field on the aperture plane and the integral is performed over the aperture plane. The contribution to spillover due solely to the primary is then determined by

$$\eta_{S,\text{pri}} = \frac{\eta_S}{\eta_{S,\text{sub}}}. \quad (25)$$

#### 4.2.2 Blockage efficiency, $\eta_B$

The blockage efficiency can be approximated by examining the projected blocked area on the aperture plane. The ray tracing procedure produces a mask specifies if any portion of a given ray is blocked by a strut, or intersects the hole in the primary. Small objects, such as struts, in practice have a different electrical cross section than geometric cross section, and this cross section is polarization dependent. Here we make the ray trace approximation, which produces reasonably accurate results, except for wavelengths that are larger than, or similar in size to, the smallest significant blocking structures. The standard expression for blockage efficiency is used:

$$\eta_B = \frac{\left| \int_{\text{aper}} \vec{E}(x, y) M(x, y) dA \right|^2}{\left| \int_{\text{aper}} \vec{E}(x, y) dA \right|^2}. \quad (26)$$

Here  $M(x, y)$  is the mask expression that has a value of 1 for an unblocked location on the aperture, and 0 for a blocked region. This formulation allows for partially blocked cells to be numerically integrated.

#### 4.2.3 Surface roughness efficiency, $\eta_\sigma$

A surface that has roughness will contribute to random scattering and hence loss of efficiency. Without derivation we state the surface roughness efficiency as derived by Ruze (1966):

$$\eta_\sigma = e^{-\left(\frac{4\pi\epsilon}{\lambda}\right)^2}. \quad (27)$$

The RMS surface error,  $\epsilon$ , represents contributions from both the primary and secondary surface; the individual surface errors add in quadrature. It should be noted that this equation is strictly true only for normal incidence. Deep dishes (i.e.,  $f/D < 1$ ) may see deviations from this estimate since the normal incidence approximation breaks down.

#### 4.2.4 Illumination efficiency, $\eta_I$

An aperture that has uniform amplitude and phase illumination will produce a beam with the greatest directivity. The illumination, or aperture, efficiency is a measure of the efficiency of a radiating aperture relative to the uniformly illuminated aperture. Again without derivation, the expression used to compute the illumination efficiency is

$$\eta_I = \frac{\left| \int_{\text{aper}} \vec{E}(x, y) M(x, y) dA \right|^2}{A_m \int_{\text{aper}} |E^2(x, y)| M^2(x, y) dA}, \quad (28)$$

where  $A_m$  is the *masked area*,

$$A_m = \int_{\text{aper}} M(x, y) dA. \quad (29)$$

Often the this illumination efficiency is decomposed into factors that are due to amplitude  $\eta_{\text{I,amp}}$  and phase  $\eta_{\text{I,phase}}$  with the corresponding values:

$$\eta_{\text{I,amp}} = \frac{\left[ \int_{\text{aper}} |E(x, y)| M(x, y) dA \right]^2}{A_{\text{m}} \int_{\text{aper}} |E^2(x, y)| M^2(x, y) dA} \quad (30)$$

$$\eta_{\text{I,phase}} = \frac{\left| \int_{\text{aper}} \vec{E}(x, y) M(x, y) dA \right|^2}{\left[ \int_{\text{aper}} |E(x, y)| M(x, y) dA \right]^2}. \quad (31)$$

#### 4.2.5 Diffraction efficiency, $\eta_{\text{D}}$

It should be mentioned immediately that the diffraction efficiency calculation is likely wrong. An equation was empirically derived that is probably approximately correct for the VLA. A scale factor has been applied that allows antennas with different subreflector sizes to be used. This assumes that all diffraction loss is due to the subreflector, which is likely a good guess. Note that this efficiency does not currently depend on taper – another indication of its inadequacy.

#### 4.2.6 Miscellaneous efficiency, $\eta_{\text{M}}$

This final efficiency category contains everything else. The user must supply a value in the input file, otherwise 100% is assumed.

#### 4.2.7 System Temperature

The zenith system temperature is computed by determining the fraction of transmitted power that would hit the ground,  $f_{\text{g}}$ , and sky,  $f_{\text{s}} \equiv 1 - f_{\text{g}}$ , and multiplying each by their respective temperatures. The receiver temperature is then added:

$$T_{\text{sys}} = T_{\text{rec}} + f_{\text{g}} T_{\text{g}} + f_{\text{s}} T_{\text{s}}. \quad (32)$$

For a Cassegrain antenna, the fractional power hitting the ground is computed as

$$f_{\text{g}} = (1 - \eta_{\text{S,sub}}) + f(1 - \eta_{\text{B,leg}}), \quad (33)$$

where  $\eta_{\text{B,leg}}$  is the leg blockage efficiency and  $f$  is a fudge factor. The first term represents the power that spills over the primary, and thus hits the ground. The second term represents the power that scatters off the struts to the ground. The fraction of scattered power that hits the ground is controlled by  $f$ . The input parameter to set  $f$  is called **leggroundscatter**.

### 4.3 Beam calculation

Once the aperture plane electric field is known, the far field radiation pattern can be determined. For each hand of circular polarization, the following operations are performed. Fraunhofer diffraction applies as we are interested in the far field radiation pattern and the electric field is known over an entire surface (it is zero outside the aperture and computed on the aperture). The radiation at a location  $\vec{x}$  is given by

$$\vec{E}(\vec{x}) = \frac{ie^{ikr}}{2\pi r} \vec{k} \times \int_{\text{aper}} \hat{z} \times \vec{E}(x', y') e^{-i(k_x x' + k_y y')} dA', \quad (34)$$

which is adapted to our application from Eqn. 9.156 of Jackson. In this expression,  $r = |\vec{x}|$  and  $\vec{k}$  is the wave vector of the transmitted radiation. The primed coordinates refer to the coordinates on the aperture plane; the unprimed coordinates refer to the field test points. Since the integral in this case is over a uniformly

gridded plane, the integral,  $\vec{I}(l, m)$ , becomes a two-dimensional component-by-component forward<sup>4</sup> FFT of  $\hat{z} \times \vec{E}$ . Here  $(l, m)$  are the sine-projected angular sky coordinates equal to  $(x/z, y/z)$ . This is taken in the limit that  $z$  is very large. In order to reexpress Eqn. 34 in a circularly polarized basis, the radiated electric field is projected on the circular polarization basis. Thus, modulo the complex constant, the quantities of interest are:

$$E_R(l, m) = \mathbf{e}_R^* \cdot \vec{k} \times \vec{I} \quad (35)$$

$$E_L(l, m) = \mathbf{e}_L^* \cdot \vec{k} \times \vec{I}. \quad (36)$$

The vector triple product can be rearranged, and Eqns. 8 and 9 can be used simplify these to

$$E_R(l, m) = ik \mathbf{e}_R^* \cdot \vec{I} \quad (37)$$

$$E_L(l, m) = -ik \mathbf{e}_L^* \cdot \vec{I}. \quad (38)$$

## A Input file

This appendix contains a sample input file for cassbeam. This file describes in detail the geometry for an EVLA antenna at 10.0 GHz. Note that this may not in fact truly represent the geometry of the EVLA – it is meant as an example only.

```
# X-mid.in -- an input file for simulating mid X-band with EVLA
name = EVLA
# EVLA geometry
sub_h = 8.47852      # meters from vertex to subreflector
feed_x = 0.97536     # meters from optic axis to feed ring
feed_y = 0.0         # Note that the position on the feed ring is not right
feed_z = 1.67640     # height of feed ring from vertex
geom = vla_geom      # file containing the primary surface profile
feedtaper = 13.0     # dB below peak
feedthetamax = 9.26  # degrees
legwidth = 0.27      # meters wide
legfoot = 7.55       # meters from optic axis at dish
legapex = 10.93876   # meters above vertex
hole_radius = 2.0    # meters -- radius of unpanelled area
roughness=0.00035    # meters RMS error of combined surfaces
# Abnormalities specific to mid-X band
focus=-0.289        # the phase center is below the feed circle
dsub_z=-0.005        # the subreflector is moved to compensate for this
# Running parameters
freq = 10.0          # GHz
gridsize = 100       # pixels on a side
Trec=18
out = X-mid
```

## B Primary profile input file

This appendix contains a sample file containing the profile of the primary surface. Note that only a portion of the file is shown. 1240 lines have been omitted and replaced with ellipses. The first column is the radial coordinate  $r$  in meters. The second column is the axial coordinate  $z$ , also in meters. The third column is the local derivative  $dz/dr$ .

---

<sup>4</sup>A forward transform as defined in the FFT package called FFTW.

```

0.000000 0.000000 0.000000
0.010000 0.000003 0.000561
0.020000 0.000011 0.001122
0.030000 0.000025 0.001683
0.040000 0.000045 0.002244
0.050000 0.000070 0.002805
0.060000 0.000101 0.003366
0.070000 0.000137 0.003927
.
.
.
12.480000 4.311402 0.671823
12.490000 4.318122 0.672216
12.500000 4.324847 0.672607

```

## C Sample session

This appendix contains an example of the text output when running `cassbeam`.

```

parallax<365>% cassbeam X-mid.in
Antenna: VLA 0x80aba60
  freq    = 10.000000 GHz  lambda = 0.029979 m
  Tsky    = 3.000000 K Tground = 290.000000 K Trec = 18.000000 K
  dir     = -0.000000e+00 0.000000e+00 1.000000e+00
  feeddir = -0.142041, 0.000000, 0.989861
  ftaper  = 13.000000
  thmax   = 9.260000

```

```

Pathology: 0x80ac608
  subrot = Matrix (3 by 3)
    1.000000    0.000000    0.000000
    0.000000    1.000000    0.000000
    0.000000    0.000000    1.000000
  feedrot = Matrix (3 by 3)
    1.000000    0.000000    0.000000
    0.000000    1.000000    0.000000
    0.000000    0.000000    1.000000
  subshift = 0.000000e+00 0.000000e+00 -5.000000e-03
  subrotpoint = 0.000000e+00 0.000000e+00 8.478520e+00
  feedshift = 0.000000e+00 0.000000e+00 0.000000e+00

```

```

Output: 0x80ae2f8
  Spillover eff = 0.922563
  primary      = 0.997158
  subreflector = 0.925193
  Blockage eff = 0.857039
  Surface eff  = 0.978706
  Illum eff    = 0.993388
  phase eff    = 0.994786
  amp eff      = 0.998595
  Diffract eff = 0.977420

```



```

Misc eff      = 1.000000
Total eff     = 0.751363
Gain          = 5156891.55 = 67.12 dBi
Tsys          = 24.419 K
  ground      = 3.454 K
  sky         = 2.964 K
  rec         = 18.000 K
Aeff          = 368.824311 m^2
Aeff/Tsys     = 15.104166 m^2/K
l beamshift   = -0.000115 deg
m beamshift   = -0.000000 deg
l beam FWHM   = 0.070499 deg
m beam FWHM   = 0.070676 deg
Peak sidelobe = 0.039489 = -14.035194 dB

```

Output image scale is 0.002147 deg/pixel

## D References

- Born, M. & Wolf, E., “Principles of Optics: Electromagnetic Theory of Propagation, Interference and Diffraction of Light,” 6th edition, FIXME...
- Frigo, M., & Johnson, S. G., “The Fastest Fourier Transform in the West,” <http://www.fftw.org/>.
- Hamaker, J. P., Bregman, J. D., & Sault, R. J., “Understanding Radio Polarimetry, I. Mathematical Foundations,” 1996, Astronomy & Astrophysics Supplemental Series, 117, pp. 137-147.
- Jackson, J. D., “Classical Electrodynamics,” 2nd edition, 1975, Wiley.
- Ruze, J., “Antenna Tolerance Theory – A Review,” 1966, Proceedings of IEEE, vol. 54, no. 4.
- Thompson, A. R., Moran, J. M., & Swenson, G. W. Jr., “Interferometry and Synthesis in Radio Astronomy,” 2nd edition, 2001, Wiley Interscience.